Published in final edited form as:
Anal Chem. 2013 October 1; 85(19): 9173–9180. doi:10.1021/ac401868b.

A new approach to measuring protein backbone protection with high spatial resolution using H/D exchange and electron capture dissociation

Rinat R. Abzalimov, **Cedric E. Bobst**, and **Igor A. Kaltashov**✉
Department of Chemistry, University of Massachusetts-Amherst, Amherst, MA

Abstract

Inadequate spatial resolution remains one of the most serious limitations of hydrogen/deuterium exchange mass spectrometry (HDX MS), especially when applied to larger proteins (over 30 kDa). Supplementing proteolytic fragmentation of the protein in solution with ion dissociation in the gas phase has been used successfully by several groups to obtain near-residue level resolution. However, the restrictions imposed by the LC/MS/MS mode of operation on the data acquisition time frame makes it difficult in many cases to obtain signal-to-noise ratio adequate for reliable assignment of the backbone amide protection levels at individual residues. This restriction is lifted in the present work by eliminating the LC separation step from the workflow and taking advantage of the high resolving power and dynamic range of a Fourier transform ion cyclotron resonance mass spectrometer (FT ICR MS). A residue-level resolution is demonstrated for a peptic fragment of a 37 kDa recombinant protein (N-lobe of human serum transferrin) using electron-capture dissociation as an ion fragmentation tool. The absence of hydrogen scrambling in the gas phase prior to ion dissociation is verified using redundant HDX MS data generated by FT ICR MS. The backbone protection pattern generated by direct HDX MS/MS is in excellent agreement with the known crystal structure of the protein, but also provides information on conformational dynamics, which is not available from the static X-ray structure.

Introduction

Hydrogen/deuterium exchange mass spectrometry (HDX MS) has evolved in the past decade into a powerful technique capable of providing valuable information on higher order structure and dynamics of proteins ranging from small polypeptides to monoclonal antibodies and beyond.[1–4] It is now actively used to address a wide range of questions ranging from the most fundamental aspects of protein folding[5–9] to applied questions related to behavior of biotechnology products.[10–13] Despite this very impressive success record, the utility of HDX MS is frequently limited due to inadequate spatial resolution, which is determined by the size of the peptide fragments produced by proteolytic cleavage of the protein under the slow exchange conditions.[14] Although in some cases this problem can be mitigated at least to some extent by analyzing deuterium content of partially overlapping peptide fragments (which allows a residue-level resolution to be achieved in some favorable cases[15]), alternative approaches have been actively sought in the past several years to address this problem. For example, several groups pursued the so-called “top-down” HDX MS,[16] where the protein fragmentation step is outsourced from solution to the gas phase (and is implemented using either rapid collisional activation or electron-based dissociation techniques). The latter offer several important advantages, including dramatically improved

✉address correspondence to: Igor A. Kaltashov, Department of Chemistry, University of Massachusetts-Amherst, 710 North Pleasant Street, LGRT 104, Amherst, MA 01003, Tel: (413) 545-1460, Fax: (413) 545-4490, Kaltashov@chem.umass.edu.

sequence coverage under conditions preventing hydrogen scrambling prior to the ion dissociation event.[17–20] Although in some cases top-down HDX MS allows a single residue-level resolution to be achieved, the technique is currently limited to proteins of modest size (below 20 kDa).

An alternative approach (initially proposed by Smith[21] and Deinzer[22]) sought to combine proteolytic digestion in solution and peptide ion fragmentation in the gas phase. While these initial efforts met only with partial success due to the occurrence of hydrogen scrambling within peptide ions during collisional activation (an ion dissociation technique of choice at the time), a later reincarnation of this idea (which relied on electron-transfer dissociation, ETD, to fragment peptide ions in the gas phase) was more successful.[23] Several groups have used this approach to attain a near residue-level resolution in HDX MS/MS measurements on proteins in the 10–30 kDa molecular weight range.[23–25] These experiments are carried out in the LC/MS/MS mode with LC operating in the "fast mode" (shortened gradient to minimize back-exchange prior to MS measurements). As a result of that, data acquisition time for each set of fragment ions derived from a particular precursor ion is limited by the width of the elution window of a corresponding peptide. An unfortunate consequence of this is possible deviation of the isotopic distribution of the fragment ions from those that truly reflect their isotopic make-ups. Since the distribution of deuterium across the polypeptide backbone (*i.e.*, $^{1}H/^{2}H$ occupancy ratio for each backbone amide nitrogen atom) is determined by calculating the difference in deuterium content of c_{n+1} and c_n (or z_{k+1} and z_k) fragment ions, even modest errors in reading the deuterium content of the fragment ions may result in very significant errors of individual amide protection levels. The situation is expected to be particularly dire for larger proteins, since a large number of co-eluting peptides inevitably results in signal suppression for many of them, further decreasing the signal-to-noise ratio and the quality of isotopic distributions of fragment ions.

The quality of isotopic distributions in MS (also referred to as statistical characteristics or primarily variance in the intensities of the isotopic peaks) depends on the number of detected ions.[26] Unfortunately, the number of peptide ions cannot be increased arbitrarily in HDX MS measurements, since the protein sample is diluted twice prior to the digestion (first 10–100 times dilution to initiate the exchange, and second at least 2 times dilution to quench the exchange reaction). An alternative approach to enhancing the statistical characteristics of isotopic distributions would seek to increase the data acquisition time (which is universally employed to increase the signal-to-noise ratio in analytical measurements); however, the data acquisition window in a classical HDX MS scheme is limited by the chromatographic parameters (elution window) of the peptides in LC. In this work, we have been able to circumvent this problem by eliminating the LC separation step from the workflow and instead relying on the high resolving power and dynamic range of a Fourier transform ion cyclotron resonance (FT ICR) mass spectrometer to mass-select the peptide ion of interest from the mixture of proteolytic fragments and obtain the fragment ions with the quality of isotopic distributions sufficient for confident mapping of the deuterium distribution across the backbone at a single-residue resolution.

Materials and Methods

The iron-saturated N-lobe of human serum transferrin was provided by Prof. Anne B. Mason (University of Vermont College of Medicine, Burlington, VT); a 50 □M stock solution of the protein in 20 mM ammonium acetate (pH adjusted to 7.5) was used for HDX MS/MS measurements. Pepsin was purchased from Sigma-Aldrich Chemical Co. (St. Louis, MO), and D_2O was purchased from Cambridge Isotopes, Inc. (Andover, MA). All other chemicals used in this work were of analytical grade or higher. The HDX reactions with subsequent quenching and protein digestion were carried out using a doublemixing continuous flow

apparatus consisting of two silicon chip-based NanoMixers (Upchurch Scientific Inc., Oak Harbor, WA) each with a flow path volume of 60 nL, and high-precision multi-channel syringe pump Nexus-3000 (Chemyx Inc., Stafford, TX). The use of NanoMixers designed for efficient mixing of laminar flows and the high precision of solvent delivery by the syringe pump Nexus-3000 allowed the on-line experiments to be conducted at very low flow rates. HDX reactions were initiated by rapid mixing of the stock protein H_2O-solution (delivered at a flowrate of 15 μL/hr) and the D_2O-based exchange solvent (delivered at 150 μL/hr) to the first NanoMixer. Quench step with subsequent digestion was initiated by introducing low pH, low temperature quench solution of pepsin into the second NanoMixer (delivered at 150 μL/hr). The duration of the protein exposure to the exchange solvent (time interval between the two mixing events, determined by the length of the exchange loop and the flow rate) could be extended up to 30 min.

A solution containing a mixture of peptic fragments and pepsin was continuously infused into the electrospray ionization (ESI) source of SolariX 7 (Bruker Daltonics, Billerica, MA) FT ICR mass spectrometer equipped with a quadrupole front-end and a 7.0 T superconducting magnet. Peptide ions of interest were mass-selected by the quadrupole mass filter and transmitted to ICR cell of the mass spectrometer, where electron capture dissociation (ECD) was used to induce their dissociation. The following ECD parameters were used: lens voltage, 10 V; bias, 0.8 V; and pulse length, 100 msec. In order to minimize vibrational excitation of peptide ions prior to ECD, ion source temperature, declustering potentials and time interval of ion trapping, as well as RF voltage in the collision cell were adjusted such that no *b*- or *y*-ions were present in the mass spectra of fragment ions. A transient with a 512 kb dataset size was typically used for data acquisition, providing mass resolving power of at least 80,000. The deuterium content of each fragment ion was calculated based on the centroids of their isotopic distributions, and deuterium occupancy of individual amide groups was calculated by comparing deuterium contents of two *c*- or *z*-fragments that differ from each other by one amino acid residue.

Results and Discussion

The classical bottom-up approach to measuring protein dynamics locally (at the peptide level) utilizes an LC/MS scheme (where the exchange reactions are quenched, and the labeled protein is digested with an acidic protease(s) under the slow exchange conditions, followed by separation of peptic fragments with reversed-phase LC and on-line MS detection, allowing the number deuterons to be counted in each peptic fragment). The first high-resolution HDX MS measurements reported by other groups were also done in the LC/MS (or, more precisely, LC/MS/MS) mode, where electron transfer dissociation (ETD) of peptide ions eluting from LC was used to localize deuterium atoms with high spatial resolution;[23] a similar scheme was also used in all subsequent solution phase HDX MS/MS studies reported to date.[24, 25] However, despite being a mature and commonly accepted technique in the studies of protein primary structure, LC/MS/MS must meet several additional requirements when used in HDX MS studies. First, peptide ion desolvation and fragmentation must be carried under conditions that do not trigger hydrogen scrambling prior to the ion dissociation event (which requires that lower gas temperature be used in the ESI interface and the collisional heating be minimized prior to and during ion selection for subsequent fragmentation). This usually has a devastating effect on both the abundance of the precursor ion and its fragmentation efficiency (an example is shown in Figure S1 in the Supplementary Material section). Second, the fast LC commonly used in HDX MS schemes to minimize back-exchange prior to MS measurements has very narrow elution windows, which can accommodate only a very limited number of MS scans (five MS/MS scans in addition to a “survey” MS1 scan with the instrument used in this work). Finally, accurate localization of deuterium atoms across the peptide backbone requires high-quality isotopic

distributions for all fragment ions as an input, and the adequate ion statistics can only be achieved when the number of detected ions is sufficiently high. This third requirement is in obvious conflict with the first two, explaining our inability to obtain useful HDX LC/MS/MS data in the scrambling-free regime (see Figure S1 in the Supplementary Material section).

Although the ETD and/or ECD fragment ions are not abundant when the experiments are carried out under conditions minimizing hydrogen scrambling in the gas phase, adequate ion statistics (and, subsequently, reliable isotopic distributions of fragment ions) can be achieved when the ionic signal is averaged over a prolonged period of time. This, of course, is impossible to do in the LC/MS/MS mode (where the acquisition window is limited by the duration of the peptide elution), which prompted us to examine the possibility of carrying out such measurements without LC separation of peptide fragments. Modern MS instrumentation provides excellent dynamic range, meaning that even less abundant peptide ions can be isolated from a crowded mass spectrum, and subsequently interrogated with tandem mass spectrometry. Insufficient signal-to-noise ratio can almost always be improved by increasing the data acquisition window, which is no longer limited by the parameters of the chromatographic step (see Supplementary Material for more detail). Elimination of the chromatographic separation from the experimental scheme provides an additional benefit of reducing the extent of back exchange not only by reducing the overall exposure time of peptic fragments to the “slow exchange” buffer prior to MS measurements from a typical 5–20 min. to only 30 sec., but also by eliminating their exposure to the hydrophobic C18 media (which has been shown to accelerate back exchange in HDX MS measurements during the LC step[27]).

One unfortunate feature of eliminating the LC step from the experimental scheme would be the need to carry out MS/MS measurements for each peptic fragment separately, which would result in a notable increase of the amount of time needed to provide complete coverage of the protein sequence. However, it is important to remember that obtaining a residue-level resolution for all protein segments may not be (and frequently is not) necessary. Most proteins typically display a wide spectrum of conformational dynamics across their sequence, and in a typical HDX experiment a number of peptic fragments would exhibit either very fast or very slow exchange. Further interrogation of such peptides by methods of MS/MS will not generate any additional useful information, as a fully exchanged peptide will obviously have complete replacement of hydrogen atoms with deuterium at every amide (likewise, a completely protected peptide will have full protection at every residue). On the other hand, a set of peptides that exhibit some “intermediate” level of protection would be good candidates for HDX MS/MS inquiry.

The number of such peptides worthy of detailed HDX MS/MS investigation will, of course, vary from one protein to another, but it would always be smaller than the entire complement of their peptic fragments. Furthermore, this number could be reduced even further by limiting the extent of proteolysis such that relatively long peptic fragments are generated preferentially. Indeed, while in classical HDX MS measurements an effort is usually made to generate a large number of shorter peptides (which obviously increases the spatial resolution), a limited number of relatively long peptic fragments would suffice if the deuterium distribution across their backbones can be characterized with MS/MS.

Our recent studies of conformational dynamics of the N-lobe of human serum transferrin (*h*Tf/2N)[28] and the on-going studies of the full-length human transferrin (*h*Tf)[29] provide abundant examples of peptic fragments for which complementing the classical HDX MS measurements with MS/MS would not be particularly useful (*e.g.*, peptides derived from the protein segments localized within flexible loops), and a handful of peptides for which HDX

MS data alone are not particularly meaningful, and further inquiry with MS/MS is highly desirable. One especially striking example of such a peptide is (Tyr^{71}-Val^{81}), which corresponds to a protein segment that appears to be critical for receptor binding.[29] While this peptide reveals nearly complete backbone protection on the physiologically relevant time scale (typical duration of endocytosis) when *h*Tf is bound to its cognate receptor, only an intermediate level of protection is displayed by this peptide when the exchange is carried out in the absence of the receptor.[29]

It is important to realize that "intermediate protection" could be in this case a very misleading term, as the protection may not be distributed evenly across this segment of the protein. Indeed, analysis of the crystal structure of *h*Tf/2N[30] reveals the presence of three distinct structural elements within this protein segment, namely an α-helix, a loop, and a β-strand (colored in purple, red and blue in Figure 1). While it is reasonable to expect that the middle section of this segment (the loop) should exhibit higher structural plasticity compared to the fringes (the helix and the strand), it is not clear at all if conformational dynamics of the helical section would be identical to or different from that of the β-strand section (we also note that even the notion of high structural plasticity of the loop region is not trivial, as our own recent work with a different protein produced an example of a loop displaying a remarkably high level of backbone protection[10]). The obvious importance of the structural plasticity distribution across this protein segment for the receptor recognition process, as well as the inability to deduce this distribution from the classical HDX MS measurements, make this segment an obvious candidate for "targeted" HDX MS/MS interrogation.

High-resolution HDX MS/MS characterization of conformational dynamics within the protein segment (Tyr^{71}-Val^{81}) was carried out using a continuous flow apparatus, where hydrogen exchange was initiated by rapid mixing of a protein solution (in H_2O-based solvent) and exchange buffer (20 mM NH_4Ac in D_2O at apparent pH 7.2, uncorrected for a pD effect) at a 1:10 ratio. While all flow rates were kept constant, the volume of the loop separating this mixer from the second one (which was used for rapid mixing of the protein solution with a quench buffer containing pepsin) was adjusted to provide desired exchange times (1, 5, and 25 min.). Under these conditions the average size of peptic fragments was notably larger compared to those produced in experiments that followed the classical HDX MS scheme,[28] but the extent of the sequence coverage was largely preserved (the two peptic maps are shown in Figure 1). Two peptic fragments covered the segment of interest, (Val^{67}-Phe^{84}) and (Val^{71}-Phe^{84}). Since the protection information is lost in the first residue (where amide is converted to amine) and typically compromised in the second residue (due to accelerated back-exchange under the slow exchange conditions[31]), the larger peptide was selected for subsequent HDX MS/MS interrogation.

Figure 2A shows the mass spectrum of all peptic fragments of hTf/2N produced in the course of limited digestion with pepsin under the slow exchange conditions. While the peptide of interest is a relatively minor component of the spectrum, it is nonetheless possible to isolate it for fragmentation. Although the presence of abundant peptide ions within a narrow range from (Val^{67}-Phe^{84}) led to their appearing in the isolation window (compare the inset in Figure 2A and Figure 2B), and contributing to the fragment ion signal in the MS/MS spectrum, the ECD fragments of (Val^{67}-Phe^{84}) were clearly discernible and could be easily identified (Figure 2C). Despite the significant reduction of the total ion signal, virtually unlimited data acquisition time allows the isotopic distributions of all ECD fragments to be sampled with adequate statistics. Figure 3 demonstrates how these isotopic distributions evolve as the hydrogen exchange time is changed by increasing the length of the reaction loop using two specific fragment ions (c_6^+ and z_7^+) as an example. One can clearly see that even though both fragment ions incorporate the same number of backbone

amide group, the deuterium uptake within the peptide segment represented by the c_6^+ fragment is more efficient compared to that of the segment represented by the z_7^+ fragment ion, clearly suggesting that the C-terminal part of the peptide (Val[71]-Phe[84]) has noticeably higher protection compared to its N-terminal part.

A more detailed pattern of the backbone protection can be deduced from the HDX MS/MS data by comparing the levels of deuteration of adjacent fragment ions in the *c*- and *z*-fragment ladders. For example, seven z_k^+ ions were produced upon fragmentation of the triply charged precursor ion, and analysis of their deuterium content allows a backbone protection pattern to be established at a single residue-level resolution for the peptide segment Ala[73]-Lys[78] (excluding Pro[74], which lacks a backbone amide hydrogen atom), as well as cumulative protection for the two preceding residues Tyr[71]-Leu[72] (Figure 4A). Cumulative protection was also established for the five residue-long segment Val[80]-Phe[84] based on the deuterium content of the z_7^+ fragment (the smallest *z*-fragment detected). Analysis of the deuterium content of c_n^+ fragment ions generated upon dissociation of the triply charged precursor ion (Figure 4B) yields a backbone protection pattern that is partially redundant, but also contains some additional features. For example, individual contributions of Tyr[71] and Leu[72] can be resolved, and cumulative protection of the two preceding residues Asp[69]-Ala[70] can be determined. Furthermore, the slight incongruence of the redundant data points (*i.e.*, protection at Ala[73], Asn[75], and Lys[78]) provides an estimate of the confidence level for these measurements (which was determined to be close to the experimental error derived from the standard deviation, 6%). Finally, a few *c*- and *z*-fragment ions could be derived from the doubly charged precursor ion (Figure 4C), and although their number is considerably smaller compared to the fragments derived from the triply charged precursor ion, they do contribute important non-redundant information. For example, they allow individual contributions of Ala[82], Glu[83], and Phe[84] to be determined within the previously unresolved segment Val[80]-Phe[84], and also provide individual contributions for Asp[69] and Ala[70].

Taken together, HDX MS/MS data allow the protection patterns for the peptide backbone to be determined at various time points at a single residue-level resolution (Figure 4D) with the exception of two residues (Val[80] and Ala[81], for which cumulative protection is determined). As noted earlier, the protection levels for the first two residues in the peptide sequence were not analyzed, since the first amide (at Val[67]) is converted to amine upon proteolysis, leading to a complete loss of information on its protection, while the exchange at the second amide (in our case Tyr[68]) is generally relatively fast during the slow exchange phase,[31] and the information on its protection level within the intact protein is usually lost. The only two other missing residues in the sequence are Pro[74] and Pro[79], which lack amide hydrogen atoms. The backbone protection pattern deduced from HDX MS/MS measurements carried out following 1 min exchange in solution is consistent with the available crystal structures of transferrin in that it shows robust exchange within the Leu[72]-Asn[76] segment of the peptide, which corresponds to a loop region in the crystal structure,[30] while the flanking regions corresponding to an α-helical region and a β-strand have considerably higher protection. What is more important, the HDX MS/MS measurements do not simply corroborate the high-resolution X-ray crystallographic data, but provide additional important information. For example, HDX MS/MS measurements carried out at longer exchange times (*e.g.*, 5 min) indicate significant increase of the deuterium content within the α-helical region (but not the β-strand). Furthermore, the protection pattern corresponding to the 25 min of exchange in solution shows nearly complete exchange within the helical segment, while the backbone amide hydrogen atoms within the β-strand remain largely intact. This provides clear evidence of a more dynamic character of the α-helical region compared to the β-strand, information that cannot be deduced from the crystal structure alone.

Several other peptic fragments derived from hTf/2N exhibit intermediate levels of deuterium uptake in HDX MS measurements. Given their considerable lengths, it is reasonable to assume that rather than reporting uniform exchange kinetics across all backbone amides, these cumulative levels of exchange average out dramatically different contributions from different structural elements incorporated in these segments. Two particularly interesting examples are peptic fragments (Leu^{266}-Leu^{284}) and (Phe^{295}-Met^{313}), the former incorporating a helical segment and a loop, and the latter comprising of a loop/ β-strand/loop/ α-helix sequence (see Figure S2 in the Supplementary Material section). HDX/MS/MS measurements of local deuterium occupancy within these segments do show that the amide protection is indeed distributed very unevenly across the backbone by revealing regions of low and high deuterium uptake (bottom panels in Figure S2 in the Supplementary Material section). Not surprisingly, the residues with high levels of deuterium incorporation are all localized within loop regions, while protected residues are localized within structured elements (either β-strands or α-helices).

A very important question that must be addressed each time ion fragmentation is used to enhance the spatial resolution in HDX MS measurement is the possibility of hydrogen scrambling. Extensive scrambling randomizes the distribution of deuterium labels and obviously renders the measurements meaningless. While electron-based fragmentation methods have been repeatedly shown to induce negligible scrambling,[16–18, 32, 33] collisional heating of ions that is frequently used prior to ECD or ETD to enhance the fragmentation efficiency certainly may (and was actually shown to[33]) induce scrambling within peptide or protein ions prior to their dissociation. Various approaches have been used in the past to detect the occurrence of hydrogen scrambling and estimate its extent. While the most reliable approach is a comparison between the protection patterns deduced from HDX MS/MS measurements and the structural data obtained by high-resolution NMR and/or X-ray crystallography, it obviously cannot be used when HDX MS/MS is used to probe conformation and dynamics of novel targets, for which no high-resolution structural data exist. Alternative approaches include monitoring of deuterium content of built-in "scrambling reporters," such as unstructured engineered protein segments (*e.g.*, Histags [18, 34] or other extrinsic reporters[33]), which also may not be suitable for all proteins.

In this work we had the benefit of being able to compare the protection pattern deduced from HDX MS/MS measurements to the protein crystal structure (with the two being in agreement with each other, *vide supra*); however, we note that even in the absence of the crystal structure we would have been able to prove that the hydrogen scrambling was minimal or absent altogether. First, all instrumental parameters were tuned in such a way that *b*- and *y*-fragment ions were absent from the ECD mass spectra (these ions are frequently used as indicators of the occurrence of collision-activated dissociation). Elimination of these fragment ions was achieved by adjusting the collision cell RF voltage down to 500 V (compare to the standard level of 1400 V). The potentials of both ion funnels were reduced by 20 V, the ion source temperature was kept at 50 °C (compared to the standard operating temperature of 150 °C), and the collision voltage was reduced to 1.5 V (from standard 5 V). Second, despite the absence of the built-in scrambling reporters in the protein used in our work, the extent of hydrogen scrambling could still be estimated based on redundant data sets. For example, protection maps deduced from fragment ions generated by ECD of doubly- and triply-charged peptide ions (Figure 4A-C) are consistent with each other. Furthermore, comparison of the cumulative protection levels for several protein segments deduced from overlapping peptic fragments[28] with those obtained by summing up protection of individual amides deduced from HDX MS/MS measurements also shows excellent agreement (Figure 5A). Finally, comparison of the deuterium content of a shorter peptic fragment (Tyr^{71}-Phe^{84}) with a congruent (*i.e.*, having the same set of backbone amides) fragment ion derived from a larger precursor (z_{14}^{+} generated by ECD of the peptide

considered in this work) also shows excellent agreement (Figure 5B). Therefore, it would be possible to conclude that the results of HDX MS/MS work presented in this study were unaffected by hydrogen scrambling even if the protein crystal structure were unavailable.

Even though our discussion has been focused on the analytical aspects of the presented work, it is worth mentioning that the protein segment whose backbone dynamics has been analyzed at high spatial resolution with HDX MS/MS is a very important player in both cognate ligand (ferric ion) binding by transferrin and its association with the receptor. This protein segment is unusual in that it becomes less conformationally stable upon metal ion binding,[28] while the protein as a whole becomes significantly more stable as a result of iron binding. Since this segment is "sandwiched" between two iron-coordinating residues (Asp^{63} and Tyr^{95}), we hypothesized that its anomalous behavior (increased backbone mobility in the holo-form) is a way to release the conformational strain induced by the metal ion binding and subsequent closing of the metal-binding cleft.[28] The results of the present work provide strong indication that it is the helical region of this segment that acts as a primary "stress release" element. Furthermore, the on-going HDX MS studies of transferrin binding to its cognate receptor (of which only a preliminary account has been published[29]) indicate strong involvement of this protein segment in the receptor recognition process, consistent with the binding model based on low-resolution cryo-EM structure[35] and a more recent higher resolution X-ray crystallographic study.[36] In fact, it is four residues within this segment (Tyr^{68}, Tyr^{71}, Ala^{73} and Asn^{75}) that are critical for the binding, and this motif appears to remain attached to the receptor throughout the entire cycle of endocytosis despite significant changes in conformations of both proteins.[36] The role of conformational plasticity in protein association is now widely appreciated despite being seemingly counterintuitive,[37, 38] and the flexibility of both the loop region and the helical segment of transferrin N-lobe located at the receptor interface detected in this work are undoubtedly important factors allowing this region of the protein not only to adapt easily to its binding partner at the cell surface, but also to remain bound to the receptor during various stages of endocytosis when both chemical environment and the receptor conformation undergo dramatic changes.

Conclusions

We have been able to use a combination of a classical "bottom-up" HDX MS scheme without chromatographic separation of peptic fragments and ECD as a means of peptide ion fragmentation in the gas phase to obtain high resolution maps of backbone flexibility of a key segment of transferrin N-lobe, which is critical for both metal ion and receptor binding. The size of this protein and the presence of the paramagnetic ligand (Fe^{3+}) place it well outside of the reach of high-resolution NMR spectroscopy. While the high-resolution crystal structure of this protein is available (and is in excellent agreement with the backbone flexibility pattern deduced from HDX MS/MS measurements), it provides only a static snapshot of the protein conformation without revealing any information on the backbone dynamics. Contrary to this, deuterium incorporation maps produced at a single-residue resolution following H/D exchange of varying length provide indication of a wide spectrum of conformational plasticity even within the structured protein segments. Unlike most of the published reports that take advantage of tandem mass spectrometry to complement the bottom-up HDX MS measurements carried out on the LC time scale, the new method does not employ LC separation and deals with only one (or potentially a handful) of peptic fragments at a time. Elimination of the chromatographic separation step from the experimental scheme allows the quality of the isotopic distributions of fragment ions to be increased dramatically, and also results in a significant (*ca.* two-fold) reduction of the levels of back exchange. While the need to carry out HDX/MS/MS measurements for each peptic fragment (or a group of peptides) individually does not allow the new approach to be used in a high-throughput fashion for exhaustive characterization of the entire protein, it appears to

be ideally suited for studies requiring high-resolution data on conformation and dynamics for only a limited number of protein segments (*e.g.*, monitoring interaction of biopharmaceuticals with their physiological partners and therapeutic targets[39]).

Supplementary Material

Refer to Web version on PubMed Central for supplementary material.

Acknowledgments

This work was supported by the grant R01 GM061666 from the National Institutes of Health. Acquisition of the Fourier transform ion cyclotron resonance mass spectrometer was supported by a grant CHE-0923329 from the National Science Foundation. The authors are grateful to Prof. Anne B. Mason (University of Vermont College of Medicine, Burlington, VT) for providing the N-lobe of human serum transferrin.

References

1. Engen JR. Analysis of protein conformation and dynamics by hydrogen/deuterium exchange MS. Anal Chem. 2009; 81:7870–7875. [PubMed: 19788312]
2. Konermann L, Pan J, Liu YH. Hydrogen exchange mass spectrometry for studying protein structure and dynamics. Chem Soc Rev. 2011; 40:1224–1234. [PubMed: 21173980]
3. Skinner JJ, Lim WK, Bedard S, Black BE, Englander SW. Protein dynamics viewed by hydrogen exchange. Protein Sci. 2012; 21:996–1005. [PubMed: 22544544]
4. Kaltashov IA, Bobst CE, Abzalimov RR. Mass spectrometry-based methods to study protein architecture and dynamics. Protein Sci. 2013; 22:530–544. [PubMed: 23436701]
5. Miranker A, Robinson CV, Radford SE, Dobson CM. Investigation of protein folding by mass spectrometry. FASEB J. 1996; 10:93–101. [PubMed: 8566553]
6. Jaswal SS, Miranker AD. Scope and utility of hydrogen exchange as a tool for mapping landscapes. Protein Sci. 2007; 16:2378–2390. [PubMed: 17962401]
7. Konermann L, Simmons DA. Protein-folding kinetics and mechanisms studied by pulse-labeling and mass spectrometry. Mass Spectrom Rev. 2003; 22:1–26. [PubMed: 12768602]
8. Konermann L, Tong X, Pan Y. Protein structure and dynamics studied by mass spectrometry: H/D exchange, hydroxyl radical labeling, and related approaches. J Mass Spectrom. 2008; 43:1021–1036. [PubMed: 18523973]
9. Jaswal SS. Biological insights from hydrogen exchange mass spectrometry. Biochimica et Biophysica Acta (BBA) - Proteins and Proteomics. 2013 in press. 10.1016/j.bbapap.2012.10.011
10. Bobst CE, Thomas JJ, Salinas P, Savickas P, Kaltashov IA. Impact of oxidation on protein therapeutics: Conformational dynamics of intact and oxidized acid- □glucocerebrosidase at near-physiological pH. Protein Sci. 2010; 19:2366–2378. [PubMed: 20945356]
11. Bobst CE, Abzalimov RR, Houde D, Kloczewiak M, Mhatre R, Berkowitz SA, Kaltashov IA. Detection and characterization of altered conformations of protein pharmaceuticals using complementary mass spectrometry-based approaches. Anal Chem. 2008; 80:7473–7481. [PubMed: 18729476]
12. Houde D, Berkowitz SA, Engen JR. The utility of hydrogen/deuterium exchange mass spectrometry in biopharmaceutical comparability studies. J Pharm Sci. 2011; 100:2071–2086. [PubMed: 21491437]
13. Kaltashov IA, Bobst CE, Abzalimov RR, Berkowitz SA, Houde D. Conformation and dynamics of biopharmaceuticals: transition of mass spectrometry-based tools from academe to industry. J Am Soc Mass Spectrom. 2010; 21:323–337. [PubMed: 19963397]
14. Ahn J, Cao M-J, Yu YQ, Engen JR. Accessing the reproducibility and specificity of pepsin and other aspartic proteases. Biochimica et Biophysica Acta (BBA) - Proteins and Proteomics. 2013 in press. 10.1016/j.bbapap.2012.10.003
15. Del Mar C, Greenbaum EA, Mayne L, Englander SW, Woods VL Jr. Structure and properties of □-synuclein otheramyloids determined at the amino acid level. Proc Natl Acad Sci U S A. 2005; 102:15477–15482. [PubMed: 16223878]

16. Kaltashov IA, Bobst CE, Abzalimov RR. H/D exchange and mass spectrometry in the studies of protein conformation and dynamics: Is there a need for a top-down approach? Anal Chem. 2009; 81:7892–7899. [PubMed: 19694441]

17. Pan J, Han J, Borchers CH, Konermann L. Hydrogen/deuterium exchange mass spectrometry with top-down electron capture dissociation for characterizing structural transitions of a 17 kDa protein. J Am Chem Soc. 2009; 131:12801–12808. [PubMed: 19670873]

18. Abzalimov RR, Kaplan DA, Easterling ML, Kaltashov IA. Protein conformations can be probed in top-down HDX MS experiments utilizing electron transfer dissociation of protein ions without hydrogen scrambling. J Am Soc Mass Spectrom. 2009; 20:1514–1517. [PubMed: 19467606]

19. Pan J, Han J, Borchers CH, Konermann L. Conformer-specific hydrogen exchange analysis of A (1–42) oligomers by top-down electron capture dissociation mass spectrometry. Anal Chem. 2011; 83:5386–5393. [PubMed: 21635007]

20. Pan J, Borchers CH. Top-down structural analysis of posttranslationally modified proteins by Fourier transform ion cyclotron resonance-MS with hydrogen/deuterium exchange and electron capture dissociation. Proteomics. 2013; 13:974–981. [PubMed: 23319428]

21. Deng YZ, Pan H, Smith DL. Selective isotope labeling demonstrates that hydrogen exchange at individual peptide amide linkages can be determined by collision-induced dissociation mass spectrometry. J Am Chem Soc. 1999; 121:1966–1967.

22. Kim MY, Maier CS, Reed DJ, Deinzer ML. Site-specific amide hydrogen/deuterium exchange in *E. coli* thioredoxins measured by electrospray ionization mass spectrometry. J Am Chem Soc. 2001; 123:9860–9866. [PubMed: 11583550]

23. Rand KD, Zehl M, Jensen ON, Jorgensen TJD. Protein hydrogen exchange measured at single-residue resolution by electron transfer dissociation mass spectrometry. Anal Chem. 2009; 81:5577–5584. [PubMed: 19601649]

24. Huang RYC, Garai K, Frieden C, Gross ML. Hydrogen/deuterium exchange and electron-transfer dissociation mass spectrometry determine the interface and dynamics of apolipoprotein E oligomerization. Biochemistry. 2011; 50:9273–9282. [PubMed: 21899263]

25. Landgraf R, Chalmers M, Griffin P. Automated hydrogen/deuterium exchange electron transfer dissociation high resolution mass spectrometry measured at single-amide resolution. Journal of the American Society for Mass Spectrometry. 2012; 23:301–309. [PubMed: 22131230]

26. Kaur P, O'Connor PB. Use of statistical methods for estimation of total number of charges in a mass spectrometry experiment. Anal Chem. 2004; 76:2756–2762. [PubMed: 15144185]

27. Zhang HM, Bou-Assaf GM, Emmett MR, Marshall AG. Fast reversed-phase liquid chromatography to reduce back exchange and increase throughput in H/D exchange monitored by FT-ICR mass spectrometry. J Am Soc Mass Spectrom. 2009; 20:520–524. [PubMed: 19095461]

28. Bobst CE, Zhang M, Kaltashov IA. Existence of a noncanonical state of iron-bound transferrin at endosomal pH revealed by hydrogen exchange and mass spectrometry. J Mol Biol. 2009; 388:954–967. [PubMed: 19324057]

29. Kaltashov IA, Bobst CE, Zhang M, Leverence R, Gumerov DR. Transferrin as a model system for method development to study structure, dynamics and interactions of metalloproteins using mass spectrometry. Biochim Biophys Acta. 2012; 1820:417–426. [PubMed: 21726602]

30. MacGillivray RT, Moore SA, Chen J, Anderson BF, Baker H, Luo Y, Bewley M, Smith CA, Murphy ME, Wang Y, Mason AB, Woodworth RC, Brayer GD, Baker EN. Two high-resolution crystal structures of the recombinant N-lobe of human transferrin reveal a structural change implicated in iron release. Biochemistry. 1998; 37:7919–7928. [PubMed: 9609685]

31. Bai Y, Milne JS, Mayne L, Englander SW. Primary structure effects on peptide group hydrogen exchange. Proteins. 1993; 17:75–86. [PubMed: 8234246]

32. Pan J, Han J, Borchers CH, Konermann L. Electron capture dissociation of electrosprayed protein ions for spatially resolved hydrogen exchange measurements. J Am Chem Soc. 2008; 130:11574–11575. [PubMed: 18686958]

33. Zehl M, Rand KD, Jensen ON, Jorgensen TJ. Electron transfer dissociation facilitates the measurement of deuterium incorporation into selectively labeled peptides with single residue resolution. J Am Chem Soc. 2008; 130:17453–17459. [PubMed: 19035774]

34. Abzalimov RR, Kaltashov IA. Controlling hydrogen scrambling in multiply charged protein ions during collisional activation: Implications for top-down hydrogen/deuterium exchange MS utilizing collisional activation in the gas phase. Anal Chem. 2010; 82:942–950. [PubMed: 20055445]

35. Cheng Y, Zak O, Aisen P, Harrison SC, Walz T. Structure of the human transferrin receptor-transferrin complex. Cell. 2004; 116:565–576. [PubMed: 14980223]

36. Eckenroth BE, Steere AN, Chasteen ND, Everse SJ, Mason AB. How the binding of human transferrin primes the transferrin receptor potentiating iron release at endosomal pH. Proc Natl Acad Sci U S A. 2011; 108:13089–13094. [PubMed: 21788477]

37. Mittag T, Kay LE, Forman-Kay JD. Protein dynamics and conformational disorder in molecular recognition. Journal of Molecular Recognition. 2010; 23:105–116. [PubMed: 19585546]

38. Vistoli G, Pedretti A, Testa B. Chemodiversity and molecular plasticity: recognition processes as explored by property spaces. Future Medicinal Chemistry. 2011; 3:995–1010. [PubMed: 21707401]

39. Kaltashov IA, Bobst CE, Nguyen SN, Wang S. Emerging mass spectrometry-based approaches to probe protein-receptor interactions: Focus on overcoming physiological barriers. Adv Drug Deliv Rev. 2013; 65:1020–1030. [PubMed: 23624418]

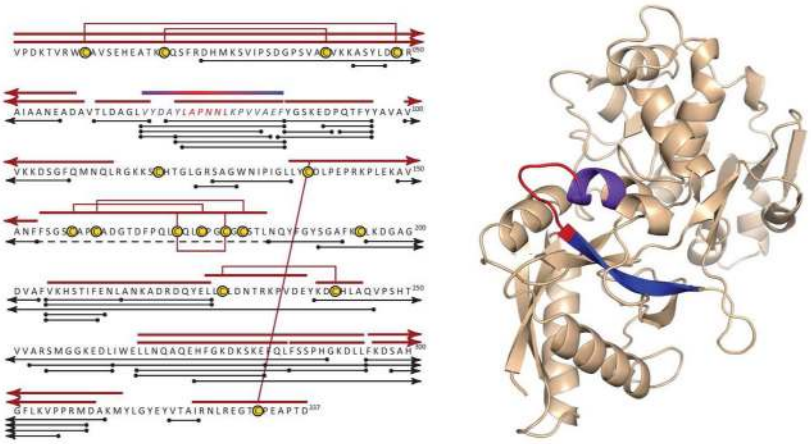

Figure 1.

Primary (left) and tertiary (right) structures of *h*Tf/2N. The peptic maps obtained in the present work and using classical HDX MS set-up are shown with brown and black lines, respectively. The secondary structure of the peptic fragment [Val^{67}-Phe^{84}] is color-coded (an α-helix, purple; a loop, red; and a β-strand, blue).

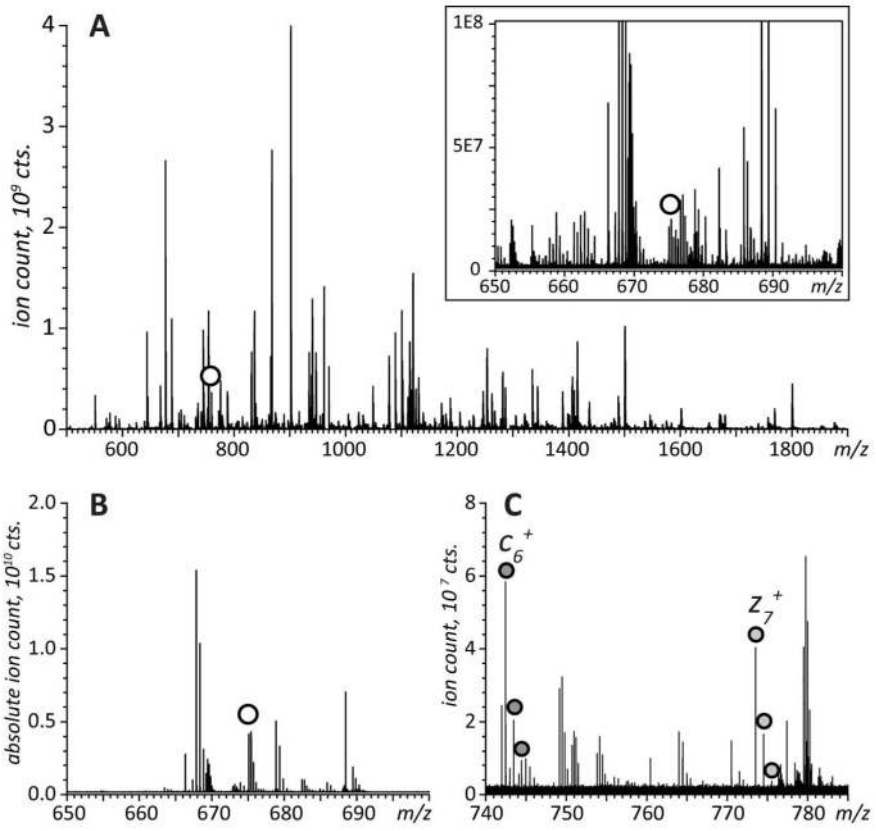

Figure 2.

A: a mass spectrum of peptic fragments of hTf/2N acquired with a continuous-flow apparatus. The inset shows a region of the spectrum containing ionic signal representing the (Val^{67}-Phe^{84}) peptide (charge state +2, labeled with an open circle). **B**: Ionic signal after mass-isolation of the peptide of interest. **C**: a fraction of the spectrum of ECD fragments of isolated ions showing c_6^+ and z_7^+ fragments of peptide ion [Val^{67}-Phe^{84}].

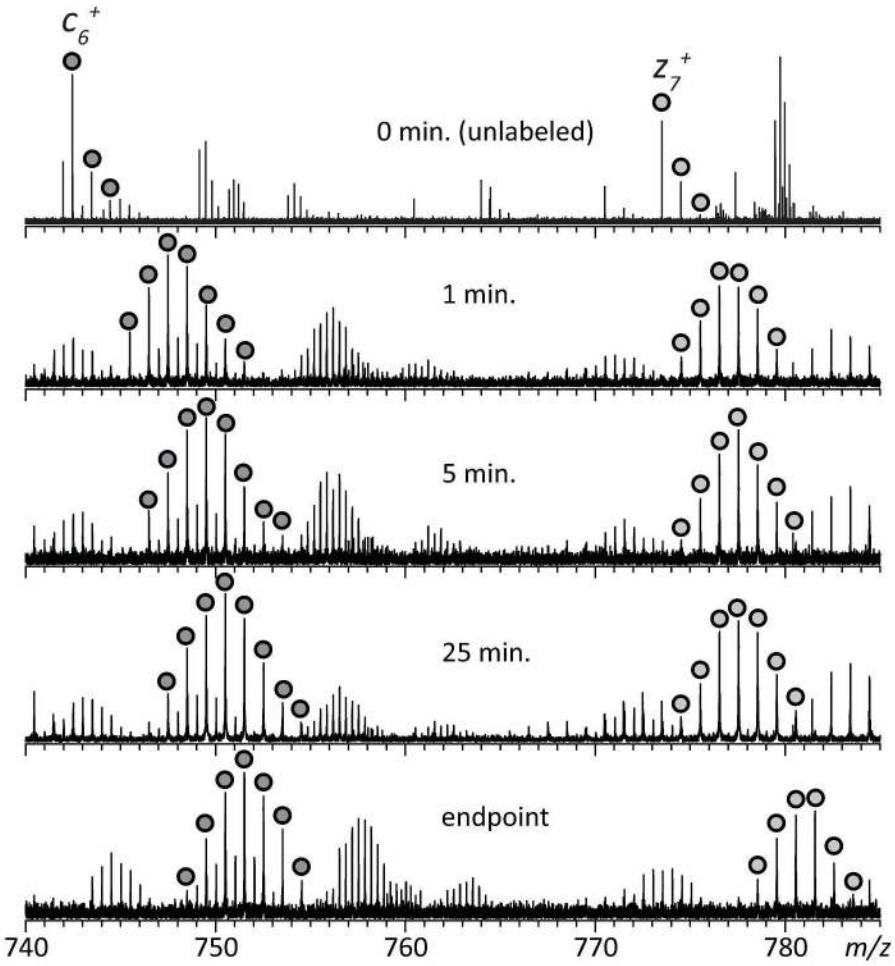

Figure 3.
Evolution of isotopic distribution of c_6^+ and z_7^+ fragments produced upon ECD of the precursor ion representing the doubly protonated form of peptide (Val^{67}-Phe^{84}).

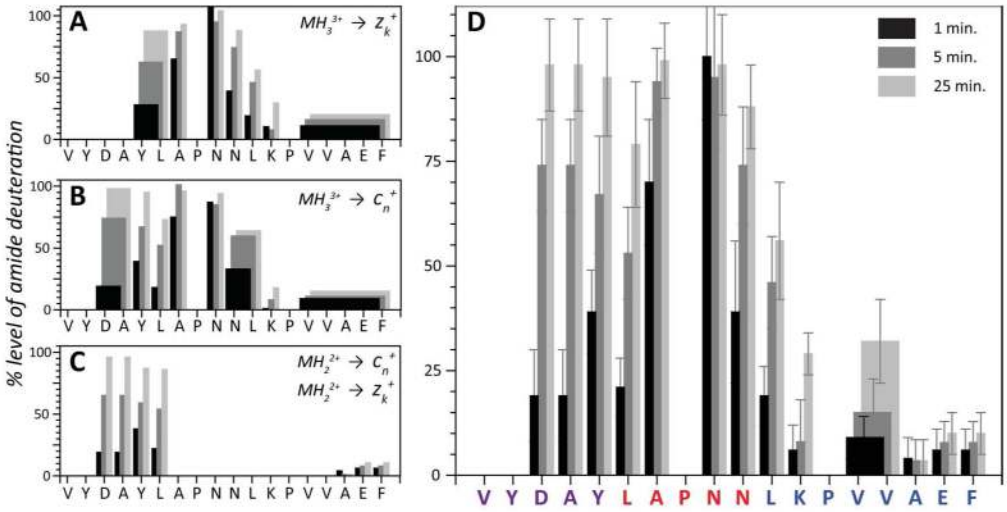

Figure 4.

Backbone protection maps deduced from a ladder of *z*- (**A**) and *c*- (**B**) fragments generated upon ECD of a triply protonated peptide (Val^{67}-Phe^{84}), and from the entire complement of ECD fragments generated upon dissociation of the doubly protonated ion representing the same peptide (**C**). Diagram **D** shows the overall protection maps that combine the data presented in panels **A**-**C**. Bars of different colors represent varying exchange time in solution (as indicated in panel **D**).

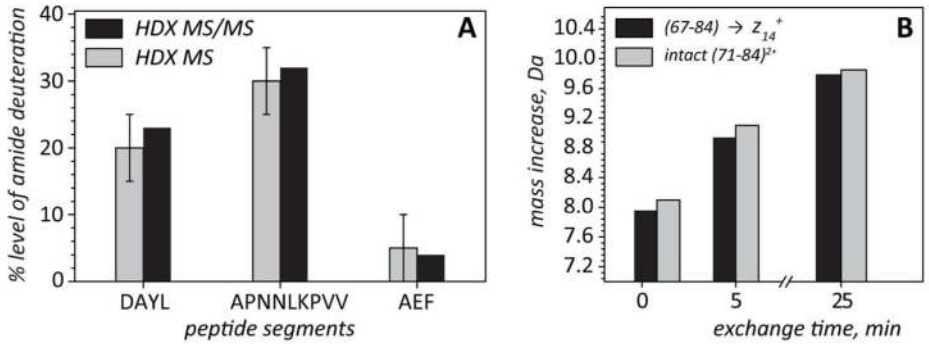

Figure 5.

A: comparison of the cumulative protection for several shorter segments within the peptic fragment (Val^{67}-Phe^{84}) obtained with HDX MS and deduced from the overlapping peptic fragments. **B**: comparison of deuterium incorporation in a shorter peptic fragment (Tyr^{71}-Phe^{84}) and a congruent fragment z_{14}^{+} derived from a longer peptic fragment (Val^{67}-Phe^{84}).